

Recovery of a Smooth Metric via Wave Field and Coordinate Transformation Reconstruction*

Maarten V. de Hoop[†], Paul Kepley[‡], and Lauri Oksanen[§]

Abstract. In this paper, we study the inverse boundary value problem for the wave equation with a view towards an explicit reconstruction procedure. We consider both the anisotropic problem where the unknown is a general Riemannian metric smoothly varying in a domain, and the isotropic problem where the metric is conformal to the Euclidean metric. Our objective in both cases is to construct the metric, using either the Neumann-to-Dirichlet (N-to-D) map or Dirichlet-to-Neumann (D-to-N) map as the data. In the anisotropic case we construct the metric in the boundary normal (or semi-geodesic) coordinates via reconstruction of the wave field in the interior of the domain. In the isotropic case we can go further and construct the wave speed in the Euclidean coordinates via reconstruction of the coordinate transformation from the boundary normal coordinates to the Euclidean coordinates. Both cases utilize a variant of the Boundary Control method, and work by probing the interior using special boundary sources. We provide a computational experiment to demonstrate our procedure in the isotropic case with N-to-D data.

Key words. inverse problem, wave equation, boundary control, Riemannian metric

AMS subject classifications. 35R30, 35L05

1. Introduction. We study the inverse boundary value problem for the wave equation from a computational point of view. Specifically, let $M \subset \mathbb{R}^n$ be a compact connected domain with smooth boundary ∂M , and let $c(x)$ be an unknown smooth strictly positive function on M . Let $u = u^f$ denote the solution to the wave equation on M , with Neumann source f ,

$$(1) \quad \begin{aligned} \partial_t^2 u - c^2(x)\Delta u &= 0, & \text{in } (0, \infty) \times M, \\ \partial_{\vec{n}} u|_{x \in \partial M} &= f, \\ u|_{t=0} = \partial_t u|_{t=0} &= 0. \end{aligned}$$

Here \vec{n} is the inward pointing (Euclidean) unit normal vector on ∂M . Let $T > 0$ and let $\mathcal{R} \subset \partial M$ be open. We suppose that the restriction of the Neumann-to-Dirichlet (N-to-D) map on $(0, 2T) \times \mathcal{R}$ is known, and denote this map by $\Lambda_{\mathcal{R}}^{2T}$. It is defined by

$$\Lambda_{\mathcal{R}}^{2T} : f \mapsto u^f|_{(0, 2T) \times \mathcal{R}}, \quad f \in C_0^\infty((0, 2T) \times \mathcal{R}).$$

*Submitted to the editors October 6, 2017.

Funding: M.V.d.H. gratefully acknowledges support from the Simons Foundation under the MATH + X program, the National Science Foundation under grant DMS-1559587, and the corporate members of the Geo-Mathematical Imaging Group at Rice University. P.K. was supported in part by the Geo-Mathematical Imaging group at Rice University. L.O. was supported by EPSRC grants EP/L026473/1 and EP/P01593X/1.

[†]Simons Chair in Computational and Applied Mathematics and Earth Science, Rice University, Houston TX 77005, USA (mdehoop@rice.edu).

[‡]Department of Mathematics, Purdue University, West Lafayette, IN 47907 (pkepley@purdue.edu).

[§]Department of Mathematics, University College London, Gower Street, London WC1E 6BT, UK (l.oksanen@ucl.ac.uk).

The goal of the inverse boundary value problem is to use the data $\Lambda_{\mathcal{R}}^{2T}$ to determine the wave speed c in a subset $\Omega \subset M$ modelling the region of interest.

Our approach to solve this inverse boundary value problem is based on the Boundary Control method that originates from [7]. There exists a large number of variants of the Boundary Control method in the theoretical literature, see e.g. the review [8], the monograph [21], and the recent theoretical uniqueness [18, 27] and stability results [12]. We face an even wider array of possibilities when designing computational implementations of the method. Previous computational studies of the method include [6, 34] and the recent work [9].

Motivated by applications to seismic imaging, we are particularly interested in the problem with partial data, that is, the case $\mathcal{R} \neq \partial M$. All known variants of the Boundary Control method that work with partial data require solving ill-posed control problems, and this appears to form the bottleneck of the resolution of the method. In this paper we consider this issue from two perspectives: we show that the steps of the method, apart from solving the control problems, are stable; and present a computational implementation of the method with a regularization for the control problems.

In addition to the above isotropic problem with the scalar speed of sound c , we consider an anisotropic problem and a variation where the data is given by the Dirichlet-to-Neumann map rather than the Neumann-to-Dirichlet map, see the definitions (2) and (3) below. We propose a computational method to reduce the anisotropic inverse boundary value problem to a problem with data in the interior of M . Analogously to elliptic inverse problems with internal data [1], this hyperbolic internal data problem may be of independent interest, and we show a Lipschitz stability result for the problem under a geometric assumption. We show the correctness of our method without additional geometric assumptions (Proposition 8), but for the stability of the internal data problem in the anisotropic case we require additional convexity condition to be satisfied (Theorem 12).

Our computational approach in the isotropic case combines two techniques that have been successfully used in the previous literature. To solve the ill-posed control problems, we use the regularized optimization approach that originates from [10]. This is combined with the use of the eikonal equation as in the previous computational studies [6, 9]. The main difference between [6, 9] and the present work is that in [6, 9] the ill-posed control problems, and the subsequent reconstruction of internal information (see Section 3 below), are implemented using the so-called wave bases rather than regularized optimization. Another distinction is that we do not rely upon the amplitude formula from geometric optics to extract internal information. Instead, we use the boundary data to construct sources that allow us to extract localized averages of waves and harmonic functions in the interior.

Our motivation to study the Boundary Control method comes from potential applications in seismic imaging. The prospect is that the method could provide a good initial guess for the local optimization methods currently in use in seismic imaging. These methods suffer from the fact that they may converge to a local minimum of the cost function and thus fail to give the true solution to the imaging problem [36]. On the other hand, the Boundary Control method is theoretically guaranteed to converge to the true solution, however, in practice, we need to give up resolution in order to stabilize the method. The numerical examples in this paper show that, when regularized suitably, the method can stably reconstruct smooth variations in the wave speed.

We reconstruct the wave speed only in a region near the measurement surface \mathcal{R} , since at least in theory, it is possible to iterate this procedure in a layer stripping fashion. The layer stripping alternates between the local reconstruction step as discussed in this paper and the so-called redatuming step that propagates the measurement data through the region where the wave speed is already known. We have developed the redatuming step computationally in [15].

We will not attempt to give an overview of computational methods for coefficient determination problems for the wave equation that are not based on the Boundary Control method. However, we mention the interesting recent computational work [3] that is based on the so-called Bukhgeim-Klibanov method [13]. We note that the Bukhgeim-Klibanov method uses different data from the Boundary Control method, requiring only a single instance of boundary values, but that it also requires that the initial data are non-vanishing. We mention also another reconstruction method that uses a single measurement [4, 5]. This method is based on a reduction to a non-linear integro-differential equation, and there are several papers on how to solve this equation (or an approximate version of it), see [25, 24] for recent results including computational implementations. Finally, we mention [20] for a thorough comparison of several methods in the 1 + 1-dimensional case.

2. Notation and techniques from the Boundary Control method. The Boundary Control (BC) method is based on the geometrical aspects of wave propagation. These are best described using the language of Riemannian geometry, and in that spirit we define the isotropic Riemannian metric $g = c(x)^{-2}dx^2$ associated to the wave speed $c(x)$ on M . Put differently, in the Cartesian coordinates of M , the metric tensor g is represented by $c(x)^{-2}$ times the identity matrix. Now the distance function of the Riemannian manifold (M, g) encodes the travel times of waves between points in M , and singular wave fronts propagate along the geodesics of (M, g) .

We will also discuss the case of an anisotropic wave speed and the Dirichlet-to-Neumann (D-to-N) map. This means that g is allowed to be an arbitrary smooth Riemannian metric on M , and we consider the wave equation

$$(2) \quad \begin{aligned} \partial_t^2 u - \Delta_g u &= 0, & \text{in } (0, \infty) \times M, \\ u|_{x \in \partial M} &= f, \\ u|_{t=0} = \partial_t u|_{t=0} &= 0 \end{aligned}$$

together with the map

$$(3) \quad \Lambda_{\mathcal{R}}^{2T} : f \mapsto -\partial_\nu u^f|_{(0, 2T) \times \mathcal{R}}, \quad f \in C_0^\infty((0, 2T) \times \mathcal{R}).$$

Here Δ_g is the Laplace-Beltrami operator on the Riemannian manifold (M, g) , and ν is the inward pointing unit normal vector to ∂M with respect to the metric g . All the techniques in this section are the same for both the isotropic and anisotropic cases and for both the choices of data N-to-D and D-to-N. The negative sign is chosen in (3) to unify the below formula (6) between the two choices of data. We leave it to the reader to adapt the formulations for the isotropic case with D-to-N and the anisotropic case with N-to-D.

The BC method is based upon approximately solving control problems of the form,

$$(4) \quad \text{find } f \text{ for which } u^f(T, \cdot) = \phi$$

where the target function $\phi \in L^2(M)$ belongs to an appropriate class of functions so that the problem can be solved without knowing the wave speed. One could call this problem a *blind control problem*. The earliest formulations of the BC method solved such control problems by applying a Gram-Schmidt orthogonalization procedure to the data. However, as noted in [10], this procedure may itself be ill-conditioned. As a result, regularization techniques were introduced to the BC method [10]. One issue that arises with this particular regularized approach to the BC method is that there is no explicit way to choose the target function ϕ . Thus in [31] a variation of the regularized approach was introduced, where the target functions ϕ were restricted to the set of characteristic functions of domains of influence. This technique uses global boundary data (i.e. $\mathcal{R} = \partial M$) to construct boundary distance functions. In [16] we introduced a modification of [31] that allowed us to localize the problem and work with partial boundary data (i.e. $\mathcal{R} \neq \partial M$). There we also studied the method computationally up to the reconstruction of boundary distance functions.

It is well-known [26] that the boundary distance functions can be used to determine the geometry (i.e. to determine the metric g up to boundary fixing isometries). While several methods to recover the geometry from the boundary distance functions have been proposed [14, 21, 22, 35], these have not been implemented computationally to our knowledge. It appears to us that, at least in the isotropic case, it is better to recover the wave speed directly without first recovering the boundary distance functions. In the next two sections, we will describe techniques that allow us to do so in both the isotropic and anisotropic cases. These will be based on the control problem setup from [16] and we will recall the setup in this section.

The difference between [16] and the present paper is that we do not use the sources f solving the control problems of the form (4) to construct boundary distance functions, instead we will use them to recover information in the interior of M . In the anisotropic case, this information is the internal data operator that gives wavefields solving (2) in semi-geodesic coordinates.

2.1. Semi-geodesic coordinates and wave caps. We consider an open subset $\Gamma \subset \partial M$ satisfying

$$\{x \in \partial M : d(x, \Gamma) \leq T\} \subset \mathcal{R},$$

where d denotes the Riemannian distance associated with g . We may replace T by a smaller time to guarantee that there exists a non-empty Γ satisfying this. In what follows we will only use the following further restriction of the N-to-D or D-to-N map

$$\Lambda_{\Gamma, \mathcal{R}}^{2T} f = \Lambda_{\mathcal{R}}^{2T} f|_{(0, 2T) \times \mathcal{R}}, \quad f \in C_0^\infty((0, 2T) \times \Gamma).$$

We now recall the definition of semi-geodesic coordinates associated to Γ . For $y \in \Gamma$, we define $\sigma_\Gamma(y)$ to be the maximal arc length for which the normal geodesic beginning at y minimizes the distance to Γ . That is, letting $\gamma(s; y, v)$ denote the point at arc length s along the geodesic beginning at y with initial velocity v , and ν the inward pointing unit normal field on Γ , we define

$$\sigma_\Gamma(y) := \max\{s \in (0, \tau_M(y, \nu)] : d(\gamma(s; y, \nu), \Gamma) = s\}.$$

We recall that $\sigma_\Gamma(y) > 0$ for $y \in \bar{\Gamma}$ (see e.g. [21, p. 50]). Defining,

$$(5) \quad x(y, s) := \gamma(s; y, \nu) \quad \text{for } y \in \Gamma \text{ and } 0 \leq s < \sigma_\Gamma(y),$$

the mapping

$$\Phi_g : \{(y, s) : y \in \Gamma \text{ and } s \in [0, \sigma_\Gamma(y))\} \rightarrow M,$$

given by $\Phi_g(y, s) := x(y, s)$ is a diffeomorphism onto its image in (M, g) , and we refer to the pair (y, s) as the semi-geodesic coordinates of the point $x(y, s)$. We note that the semi-geodesic “coordinates” that we have defined here are not strictly coordinates in the usual sense of the term, since they associate points in M with points in $\mathbb{R} \times \Gamma$ instead of points in \mathbb{R}^n . To obtain coordinates in the usual sense, one must specify local coordinate charts on Γ . Denoting the local coordinates on Γ associated with these charts by (y^1, \dots, y^{n-1}) , one can then define local semi-geodesic coordinates by (y^1, \dots, y^{n-1}, s) . We will continue to make this distinction, using the term “local” only when we need coordinates in the usual sense.

In both the scalar and anisotropic cases, our approach to recover interior information relies on computing localized averages of functions inside of M . One of the main components used to compute these averages is a family of sources that solve blind control problems with target functions of the form $\phi = 1_B$, where B is a set known as a *wave cap*. The construction of these sources will be recalled below in Lemma 2, but first we recall how wave caps are defined:

Definition 1. *Let $y \in \Gamma$, $s, h > 0$ with $s+h < \sigma_\Gamma(y)$. The wave cap, $\text{cap}_\Gamma(y, s, h)$, is defined as:*

$$\text{cap}_\Gamma(y, s, h) := \{x \in M : d(x, y) \leq s + h \text{ and } d(x, \Gamma) \geq s\}$$

See Figure 1 for an illustration.

We recall that, for all $h > 0$, the point $x(y, s)$ belongs to the set $\text{cap}_\Gamma(y, s, h)$ and $\text{diam}(\text{cap}_\Gamma(y, s, h)) \rightarrow 0$ as $h \rightarrow 0$, (see e.g. [16]). So, when h is small and ϕ is smooth, averaging ϕ over $\text{cap}_\Gamma(y, s, h)$ yields an approximation to $\phi(x(y, s))$. These observations play a central role in our reconstruction procedures.

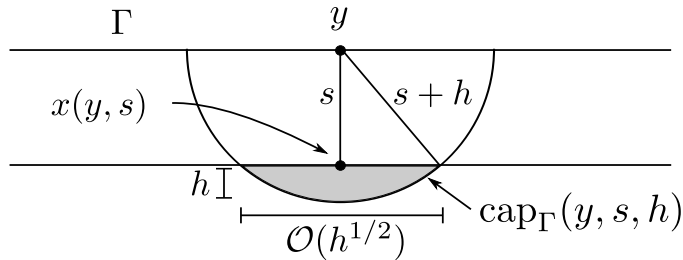


Figure 1: Geometry of a wave cap in the Euclidean case. In this case, Pythagoras’ theorem suffices to show that $\text{diam}(\text{cap}_\Gamma(y, s, h)) = \mathcal{O}(h^{1/2})$, but this is also true in general.

2.2. Elements of the BC method. As mentioned above, the BC method involves finding sources f for which $u^f(T, \cdot) \approx \phi$ for appropriate functions $\phi \in L^2(M)$. To that end, we recall the *control map*,

$$W : f \mapsto u^f(T, \cdot), \quad \text{for } f \in L^2([0, T] \times \Gamma),$$

and note that W is a bounded linear operator $W : L^2([0, T] \times \Gamma) \rightarrow L^2(M)$, see e.g. [21]. We remark that the output of W is a wave in the interior of M and hence cannot be observed directly from boundary measurements alone. Using W , one defines the *connecting operator* $K := W^*W$. The adjoint here is defined with respect to the Riemannian volume measure in the anisotropic case, and with respect to the scaled Lebesgue measure $c^{-2}(x)dx$ in the isotropic case. We denote these measures by Vol_g in both cases. In particular, we recall that K can be computed by processing the N-to-D or D-to-N map via the Blagovescenskii identity, see e.g. [30]. That is,

$$(6) \quad K = J\Lambda_\Gamma^{2T}\Theta - R\Lambda_\Gamma^T R J\Theta,$$

where $\Lambda_\Gamma^T f := (\Lambda_{\Gamma, \mathcal{R}}^T f)|_{[0, T] \times \Gamma}$, $Rf(t) := f(T - t)$ for $0 \leq t \leq T$, $Jf(t) := \int_t^{2T-t} f(s) ds$, and Θ is the inclusion operator $\Theta : L^2([0, T] \times \Gamma) \hookrightarrow L^2([0, 2T] \times \Gamma)$ given by $\Theta f(t) = f(t)$ for $0 \leq t \leq T$ and $\Theta f(t) = 0$ otherwise. We remark that the Blagovescenskii identity shows that K can be computed by operations that only involve manipulating the boundary data.

We recall some mapping properties of W that follow from finite speed of propagation for the wave equations (1) and (2). Let $\tau : \bar{\Gamma} \rightarrow [0, T]$, and define $S_\tau := \{(t, y) : T - \tau(y) \leq t \leq T\}$. Then, finite speed of propagation implies that if f is a boundary source supported in S_τ , the wavefield $u^f(T, \cdot)$ will be supported in the domain of influence $M(\tau)$, defined by

$$M(\tau) := \{x \in M : d(x, \Gamma) < \tau(y) \text{ for some } y \in \Gamma\}.$$

In turn, this implies that W satisfies, $W : L^2(S_\tau) \rightarrow L^2(M(\tau))$. So, if we define $P_\tau : L^2([0, T] \times \Gamma) \rightarrow L^2(S_\tau)$, then we can define a restricted control map $W_\tau := WP_\tau$, which satisfies $W_\tau : L^2(S_\tau) \rightarrow L^2(M(\tau))$. The point here is that, although we do not have access to the the output of W_τ , we know that the waves will be supported in the domain of influence $M(\tau)$. We also define the restricted connecting operator $K_\tau := (W_\tau)^*W_\tau = P_\tau K P_\tau$, and note that K_τ can be computed by first computing K via (6) and then applying the operator P_τ .

To construct sources that produce approximately constant wavefields on wave caps, we use a procedure from [16]. This procedure uses the fact that a wave cap can be written as the difference of two domains of influence, and requires that distances between boundary points are known. Specifically, we will suppose that for any pair $x, y \in \Gamma$ the distance $d(x, y)$ is known. As noted in [16], this is not a major restriction, since these distances can be constructed from the data Λ_Γ^{2T} . Then, using this collection of distances, we define a family of functions $\tau_y^R : \bar{\Gamma} \rightarrow \mathbb{R}_+$ by:

$$\text{for } y \in \bar{\Gamma} \text{ and } R > 0, \text{ define } \tau_y^R(x) := (R - d(x, y)) \vee 0.$$

Here we use the notation $\phi \vee \psi$ to denote the point-wise maximum between ϕ and ψ , and we will continue to use this notation below. Finally, one can show that $\text{cap}_\Gamma(y, s, h) =$

$M(\tau_y^{s+h} \vee s1_\Gamma) \setminus M(s1_\Gamma)$. We also note that, since $\partial M(\tau)$ has measure zero provided that τ is continuous on $\bar{\Gamma}$ [31], one has that $1_{\text{cap}_\Gamma(y,s,h)} = 1_{M(\tau_y^{s+h} \vee s1_\Gamma)} - 1_{M(s1_\Gamma)}$ a.e.

The following lemma is an amalgamation of results from [16], and shows that there is a family of sources $\psi_{h,\alpha}$ which produce approximately constant wavefields $u^{\psi_{h,\alpha}}(T, \cdot)$ on wave caps, and that these sources can be constructed from the boundary data $\Lambda_{\Gamma, \mathcal{R}}^{2T}$.

Lemma 2. *Let $y \in \Gamma$, $s, h > 0$ with $s + h < \sigma_\Gamma(y)$. Let $\tau_1 = s1_\Gamma$ and $\tau_2 = \tau_y^{s+h} \vee s1_\Gamma$. Define $b(t, y) := T - t$, and let $\tilde{b} = b$ in the Neumann case, and $\tilde{b} = (\Lambda_{\Gamma, \mathcal{R}}^T)^* b$ in the Dirichlet case. Then, for each $\alpha > 0$, let $f_{\alpha,i} \in L^2(S_{\tau_i})$ be the unique solution to*

$$(7) \quad (K_{\tau_i} + \alpha) f = P_{\tau_i} \tilde{b}.$$

Define,

$$(8) \quad \psi_{h,\alpha} = f_{\alpha,2} - f_{\alpha,1}.$$

Using the notation $B_h = \text{cap}_\Gamma(y, s, h)$, it holds that

$$(9) \quad \lim_{\alpha \rightarrow 0} u^{\psi_{h,\alpha}}(T, \cdot) = 1_{B_h} \quad \text{and} \quad \lim_{\alpha \rightarrow 0} \langle \psi_{h,\alpha}, P_{\tau_2} b \rangle_{L^2(S_{\tau_2})} = \text{Vol}_g(B_h).$$

We briefly sketch the proof of Lemma 2. The main idea is to approximately solve the blind control problem (4) with $\phi \equiv 1$ over the spaces $L^2(S_{\tau_i})$ for $i = 1, 2$. To accomplish this, for $i = 1, 2$, one can consider a Tikhonov regularized version of (4) depending upon a small parameter $\alpha > 0$. Then, letting $f_{\alpha,i}$ denote the minimum of the associated Tikhonov functional for $\alpha > 0$, one can obtain $f_{\alpha,i}$ by solving this functional's normal equation, given by (7). Note that all of the terms defining $f_{\alpha,i}$ in (7) can be computed in terms of the boundary data, so $f_{\alpha,i}$ can be obtained without knowing the wavespeed or metric. Appealing to properties of Tikhonov minimizers, one can then show that $W f_{\alpha,i} \rightarrow 1_{M(\tau_i)}$ as $\alpha \rightarrow 0$, and hence $W \psi_{\alpha,h} = W f_{\alpha,1} - W f_{\alpha,2} \rightarrow 1_{M(\tau_2)} - 1_{M(\tau_1)} = 1_{\text{cap}_\Gamma(y,s,h)}$, where each limit and equality holds in the L^2 sense.

3. Recovery of information in the interior. Propositions 4 and 6 below can be viewed as variants of Corollaries 1 and 2 in [10], the difference being that we use the control problem setup discussed in the previous section. One advantage of this setup is that we do not need to make the auxiliary assumption that the limit (14) in [10] is non-zero.

3.1. Wave field reconstruction in the anisotropic case. We begin with reconstruction of wavefields sampled in semi-geodesic coordinates, as encoded by the following map.

Definition 3. *Let $(y, s) \in \text{Domain}(\Phi_g)$ and $f \in L^2([0, T] \times \Gamma)$. The map $L_g : L^2([0, T] \times \Gamma) \rightarrow L^2(\text{Domain}(\Phi_g))$ is defined pointwise by*

$$(10) \quad L_g f(y, s) := u^f(T, x(y, s)).$$

We now show that L_g can be computed from the N-to-D map.

Proposition 4. *Let $f \in C_0^\infty([0, T] \times \Gamma)$. Let $t \in [0, T]$, $y \in \Gamma$ and $s, h > 0$ with $s + h < \sigma_\Gamma(y)$ and h sufficiently small. The family of sources $\{\psi_{h,\alpha}\}_{\alpha>0}$ given in Lemma 2 satisfies*

$$(11) \quad \lim_{\alpha \rightarrow 0} \frac{\langle \psi_{h,\alpha}, K f \rangle_{L^2([0,T] \times \Gamma)}}{\langle \psi_{h,\alpha}, P_\tau b \rangle_{L^2([0,T] \times \Gamma)}} = u^f(t, x(y, s)) + \mathcal{O}(h^{1/2}).$$

Proof. Applying Lemma 2, we have that

$$\lim_{\alpha \rightarrow 0} \frac{\langle \psi_{h,\alpha}, Kf \rangle_{L^2(S_\tau)}}{\langle \psi_{h,\alpha}, P_\tau b \rangle_{L^2(S_\tau)}} = \frac{\lim_{\alpha \rightarrow 0} \langle W\psi_{h,\alpha}, Wf \rangle_{L^2(M)}}{\lim_{\alpha \rightarrow 0} \langle \psi_{h,\alpha}, P_\tau b \rangle_{L^2(S_\tau)}} = \frac{\langle 1_{B_h}, u^f(T, \cdot) \rangle_{L^2(M)}}{\text{Vol}_g(B_h)}.$$

Thus it suffices to show that:

$$\langle 1_{B_h}, u^f(T, \cdot) \rangle = \text{Vol}_g(B_h) u^f(T, x(y, s)) + \text{Vol}_g(B_h) \mathcal{O}(h^{1/2}).$$

Suppose that h is sufficiently small that B_h is contained in the image of a coordinate chart (p, U) (that is, we use the convention that $p : U \subset \mathbb{R}^n \rightarrow p(U) \subset M$). We denote the coordinates on this chart by (x^1, \dots, x^n) , and also suppose that $x(y, s)$ corresponds to the origin in this coordinate chart. Since f is C_0^∞ , it follows that u^f is smooth. Thus we can Taylor expand $u^f(T, \cdot)$ in coordinates about $x(y, s) \in B_h$, giving,

$$u^f(T, x^1, \dots, x^n) = u^f(T, 0, \dots, 0) + \partial_i u^f(T, 0, \dots, 0) x^i + \sum_{|\beta|=2} R_\beta(x^1, \dots, x^n) x^\beta$$

Where R_β is bounded by the C^2 norm of $u^f(T, x^1, \dots, x^n)$ (i.e. of $u^f(T, \cdot)$ in coordinates), on any compact neighborhood K satisfying $0 \in K \subset U$. In particular we choose K such that $B_h \subset p(K)$ for h sufficiently small. Combining these expressions and using that $x(y, s)$ corresponds to 0 in U ,

$$\begin{aligned} & \left| \langle 1_{B_h}, u^f(T, \cdot) \rangle_{L^2(M)} - \text{Vol}_g(B_h) u^f(T, x(y, s)) \right| \\ & \leq C \int_{p^{-1}(B_h)} |\partial_i u^f(T, 0, \dots, 0) x^i| + \sum_{|\beta|=2} |R_\beta(x^1, \dots, x^n) x^\beta| dx^1 \dots dx^n \end{aligned}$$

Then for points $p(x) \in M$ with coordinates $x \in U$ sufficiently close to 0, there exist constants g_*, g^* such that $g_* |x|_e \leq d(p(x), 0) \leq g^* |x|_e$, where $|x|_e$ denotes the Euclidean length of the coordinate vector x in \mathbb{R}^n . So, let $x = (0, \dots, x^i, \dots, 0)$, then note that $|x^i| = |x|_e \leq (1/g_*) d(0, p(x)) \leq (1/g_*) \text{diam}(B_h)$. Thus, for h sufficiently small,

$$\begin{aligned} & |\langle 1_{B_h}, u^f(T, \cdot) \rangle_{L^2(M)} - \text{Vol}_g(B_h) u^f(T, x(y, s))| \\ & \leq \|u^f\|_{C^1(K)} C \text{diam}(B_h) \text{Vol}_g(B_h) + \|u^f\|_{C^2(K)} (C \text{diam}(B_h))^2 \text{Vol}_g(B_h) \end{aligned}$$

Finally, the discussion in [10] implies that $\text{diam}(B_h) = \mathcal{O}(h^{1/2})$, which completes the proof. \blacksquare

Corollary 5. *For each $f \in C_0^\infty([0, T] \times \Gamma)$, $L_g f$ can be determined pointwise by taking the limit as $h \rightarrow 0$ in (11). Since $C_0^\infty([0, T] \times \Gamma)$ is dense in $L^2([0, T] \times \Gamma)$ and L_g is bounded on $L^2([0, T] \times \Gamma)$, we have that $L_g f$ is determined for all $f \in L^2([0, T] \times \Gamma)$.*

Proof. First, let $f \in C_0^\infty([0, T] \times \Gamma)$. Taking the limit as $h \rightarrow 0$ in the preceding lemma shows that $L_g f(y, s)$ can be computed for any pair $(y, s) \in \text{Domain}(\Phi_g)$, and thus $L_g f$ can be determined in semi-geodesic coordinates.

Now we show that $L_g f$ can be determined for any $f \in L^2([0, T] \times \Gamma)$. First we recall that $L_g f = \Phi_g^* Wf$. Since the pull-back operator Φ_g^* just composes a function with

a diffeomorphism, and $\bar{\Gamma}$ is compact, we have that Φ_g^* is bounded as an operator $\Phi_g^* : L^2(\text{Range}(\Phi_g)) \rightarrow L^2(\text{Domain}(\Phi_g))$. Thus L_g is a composition of bounded operators, and hence $L_g : L^2([0, T] \times \Gamma) \rightarrow L^2(\text{Domain}(\Phi_g))$ is bounded. Let $f \in L^2([0, T] \times \Gamma)$ be arbitrary. Since $C_0^\infty([0, T] \times \Gamma)$ is dense in L^2 one can find a sequence $\{f_j\}_{j=1}^\infty \subset C_0^\infty([0, T] \times \Gamma)$ such that $f_j \rightarrow f$. Then, since L_g is bounded, $L_g f = \lim_{j \rightarrow \infty} L_g f_j$. \blacksquare

3.2. Coordinate transformation reconstruction in the isotropic case. The map $\Lambda_{\partial M}^T$ is invariant under diffeomorphisms that fix the boundary of M , and therefore in the anisotropic case it is not possible to compute g in the Cartesian coordinates. The same is true for the wavefields. In the isotropic case, on the other hand, it is possible to compute the map $\Phi_g(y, s)$, and in fact, the wave speed was determined in Belishev's original paper [7] by first showing that the internal data $u^f(t, x)$ can be recovered in the Cartesian coordinates, and then using the identity

$$\frac{\Delta u(t, x)}{\partial_t^2 u(t, x)} = c^{-2}(x).$$

It was later observed that the wave speed can be recovered directly from the map Φ_g without using information on the wavefields in the interior, see e.g. [6, 10]. In the present paper we will compute $\Phi_g(y, s)$ by applying the following lemma to the Cartesian coordinate functions.

Proposition 6. *Suppose that g is isotropic, that is, $g = c^{-2}(x)dx^2$. Let $\phi \in C^\infty(M)$ be harmonic, that is, $\Delta\phi = 0$. Let $t \in [0, T]$, $y \in \Gamma$, and $s, h > 0$ with $s + h < \sigma_\Gamma(y)$. Then, for h small, the family of sources $\{\psi_{h,\alpha}\}_{\alpha>0}$ given in Lemma 2 satisfies*

$$(12) \quad \lim_{\alpha \rightarrow 0} \frac{B(\psi_{h,\alpha}, \phi)}{B(\psi_{h,\alpha}, 1)} = \phi(x(y, s)) + \mathcal{O}(h^{1/2}),$$

where

$$(13) \quad B(f, \phi) = \langle f, b\phi \rangle_{L^2([0,T] \times \Gamma; dy)} - \langle \Lambda_{\Gamma, \mathcal{R}}^T f, b\partial_\nu \phi \rangle_{L^2([0,T] \times \mathcal{R}; dy)}.$$

Where $b(t) = T - t$.

Proof. The proof is analogous to that of Proposition 4 after observing that

$$\lim_{\alpha \rightarrow 0} \frac{B(\psi_{h,\alpha}, \phi)}{B(\psi_{h,\alpha}, 1)} = \frac{\langle 1_{B_h}, \phi \rangle_{L^2(M; c^{-2} dx)}}{\langle 1_{B_h}, 1 \rangle_{L^2(M; c^{-2} dx)}}.$$

To see this, it suffices to show that for ϕ harmonic and $f \in L^2([0, T] \times \Gamma)$,

$$(14) \quad B(f, \phi) = \langle u^f(T), \phi \rangle_{L^2(M; c^{-2} dx)},$$

since then

$$\lim_{\alpha \rightarrow 0} B(\psi_{h,\alpha}, \phi) = \lim_{\alpha \rightarrow 0} \langle u^{\psi_{h,\alpha}}(T), \phi \rangle_{L^2(M; c^{-2} dx)} = \langle 1_{B_h}, \phi \rangle_{L^2(M; c^{-2} dx)}.$$

This expression holds, in particular, for the special case that $\phi \equiv 1$, since constant functions are harmonic.

The demonstration of (14) is known, and is based upon the following computation,

$$\begin{aligned} \partial_t^2 \langle u^f(t), \phi \rangle_{L^2(M; c^{-2} dx)} &= \langle \Delta u^f(t), \phi \rangle_{L^2(M; dx)} - \langle u^f(t), \Delta \phi \rangle_{L^2(M; dx)} \\ &= \langle f(t), \phi \rangle_{L^2(\partial M; dy)} - \langle \Lambda f(t), \partial_\nu \phi \rangle_{L^2(\partial M; dy)}, \end{aligned}$$

where we have written $\Lambda f = u^f|_{\partial M}$. Thus, the map $t \mapsto \langle u^f(t), \phi \rangle$ satisfies an ordinary differential equation with vanishing initial conditions, since $u^f(0) = \partial_t u^f(0) = 0$. Solving this differential equation and evaluating the result at $t = T$, we get an explicit formula for $\langle u^f(T), \phi \rangle$ depending upon f and Λf :

$$(15) \quad \langle u^f(T), \phi \rangle_{L^2(M; c^{-2} dx)} = \langle f, b\phi \rangle_{L^2([0, T] \times \Gamma; dy)} - \langle \Lambda_{\Gamma, \mathcal{R}}^T f, b\partial_\nu \phi \rangle_{L^2([0, T] \times \mathcal{R}; dy)}.$$

Which completes the demonstration of (14). Notice that we only require $\Lambda f|_{\mathcal{R}}$, since, for $t \in [0, T]$, $\Lambda f(t)$ vanishes outside of \mathcal{R} by finite speed of propagation. An analogous derivation can be found in [30] (with full boundary measurements and the D-to-N map instead of the N-to-D map). ■

As in Corollary 5, letting $h \rightarrow 0$, we see that the map

$$H_c : \{\phi \in C^\infty(M); \Delta \phi = 0\} \rightarrow C^\infty(\text{Domain}(\Phi_g)), \quad H_c \phi(y, s) = \phi(\Phi_g(y, s)),$$

can be computed from the N-to-D map, where $g = c^{-2}(x)dx^2$. To see this, first recall that $\Phi_g(y, s) := \gamma(s; y, \nu)$. Since $\gamma(\cdot; y, \nu)$ is a geodesic and ν has unit-length vector with respect to the metric g , we have that $|\partial_s \Phi_g(y, s)|_g = 1$. Then, recall that for $x \in M$ and $v \in T_x M$, the length $|v|_g$ is computed by $|v|_g^2 = c(x)^{-2}|v|_e^2$, where $|v|_e$ is the Euclidean length of v . Writing $x^j, j = 1, \dots, n$, for the Cartesian coordinate functions on M , it follows that

$$(16) \quad \Phi_g(y, s) = (H_c x^1(y, s), \dots, H_c x^n(y, s)), \quad c(\Phi_g(y, s))^2 = |\partial_s \Phi_g(y, s)|_e^2.$$

Thus c can be computed in the Cartesian coordinates by inverting the first function above and composing the inverse with the second function. We will show in Section 5 that this simple inversion method is stable.

The recovery of the internal information encoded by L_g and H_c is the most unstable part of the Boundary Control method as used in this paper. The convergence with respect to h is sublinear as characterized by (11) and (12), and the convergence with respect to α is even worse. In general we expect it to be no better than logarithmic. The recent results [11, 29] prove logarithmic stability for related control and unique continuation problems, and [16] describes how the instability shows up in numerical examples.

4. Recovery of the metric tensor. Due to the diffeomorphism invariance discussed above, we cannot recover g in the Cartesian coordinates and it is natural to recover g in the semi-geodesic coordinates. This is straightforward in theory when the internal information L_g is known, and analogously to the elliptic inverse problems with internal data [1], we expect that the problem has good stability properties when suitable sources f are used. We will next describe a way to choose the sources by using an optimization technique. This technique is not stable in general, but as shown in the next section, stability holds under suitable convexity assumptions.

Lemma 7. *In any local coordinates (x^1, \dots, x^n) ,*

$$(17) \quad g^{lk}(x) = \frac{1}{2} \left(\Delta_g(x^l x^k) - x^k \Delta_g x^l - x^l \Delta_g x^k \right).$$

Proof. Let (x^1, \dots, x^n) be local coordinates on M . Write $\alpha := \sqrt{g}$. Then

$$\begin{aligned} \Delta_g(x^l x^k) &= \frac{1}{\alpha} \partial_i \left(\alpha g^{ij} \partial_j (x^l x^k) \right) \\ &= \frac{1}{\alpha} \left(\partial_i \left(\alpha g^{il} x^k \right) + \partial_i \left(\alpha g^{ik} x^l \right) \right) \\ &= g^{kl} + x^k \frac{1}{\alpha} \partial_i \left(\alpha g^{il} \right) + g^{lk} + x^l \frac{1}{\alpha} \partial_i \left(\alpha g^{ik} \right) \\ &= 2g^{lk} + x^k \Delta_g x^l + x^l \Delta_g x^k. \end{aligned}$$

Proposition 8. *The metric g can be constructed in local semi-geodesic coordinates using the operator L_g as data.*

Proof. Let $\Omega = \text{Range}(\Phi_g)$, and $\omega \subset \Omega$ be a coordinate neighborhood for the semi-geodesic coordinates. Let (x^1, \dots, x^n) denote local semi-geodesic coordinates on ω . Fix $1 \leq j, k \leq n$ and for $\ell = 1, 2, 3$ choose $\phi_\ell \in C_0^\infty(\Omega)$, $\ell = 1, 2, 3$, such that for all $x \in \omega$,

$$(18) \quad \phi_1(x) = x^j x^k, \quad \phi_2(x) = x^j, \quad \phi_3(x) = x^k.$$

Consider the following Tikhonov regularized problem: for $\alpha > 0$ find $f \in L^2([0, T] \times \Gamma)$ minimizing

$$\|L_g f - \phi^\ell\|_{L^2(\Omega)}^2 + \alpha \|f\|_{L^2([0, T] \times \Gamma)}^2.$$

It is a well known consequence of [37], see e.g. [21], that L_g has dense range in $L^2(\Omega)$. Thus this problem has a minimizer $f_{\alpha, \ell}$ which can be obtained as the unique solution to the normal equation, see e.g. [23, Th. 2.11],

$$(19) \quad (L_g^* L_g + \alpha) f = L_g^* \phi^\ell.$$

It follows from [32, Lemma 1] that the minimizers satisfy

$$\lim_{\alpha \rightarrow 0} L_g f_{\alpha, \ell} = \phi^\ell.$$

As the wave equation (2) is translation invariant in time, we have $L_g \partial_t^2 f = \Delta_g u^f(T, \cdot)$, and therefore

$$\begin{aligned} \lim_{\alpha \rightarrow 0} \|L_g \partial_t^2 f_{\alpha, \ell} - \Delta_g \phi^\ell\|_{H^{-2}(\Omega)} &= \lim_{\alpha \rightarrow 0} \|\Delta_g (u^{f_{\alpha, \ell}}(T, \cdot) - \phi^\ell)\|_{H^{-2}(\Omega)} \\ &\leq C \lim_{\alpha \rightarrow 0} \|u^{f_{\alpha, \ell}}(T, \cdot) - \phi^\ell\|_{L^2(\Omega)} = 0. \end{aligned}$$

Thus for $\ell = 1, 2, 3$, $L_g \partial_t^2 f_{\alpha, \ell} \rightarrow \Delta_g \phi^\ell$ in the $H^{-2}(\Omega)$ sense. Using expression (17), and recalling the definitions of the target functions ϕ^ℓ , then in the local coordinates on ω we have

$$(20) \quad g^{jk} = \lim_{\alpha \rightarrow 0} \frac{1}{2} (L_g \partial_t^2 f_{\alpha, 1} - x^k L_g \partial_t^2 f_{\alpha, 2} - x^j L_g \partial_t^2 f_{\alpha, 3}),$$

where the convergence is in $H^{-2}(\omega)$. Finally, since Ω can be covered with coordinate neighborhoods such as ω , this argument can be repeated to determine g^{lk} in any local semi-geodesic coordinate chart. \blacksquare

5. On stability of the reconstruction from internal data. When discussing stability near the set Γ , we will restrict our attention to $\Omega \subset M$ and a set \mathcal{G} of smooth Riemannian metrics on M for which

$$(21) \quad \bar{\Omega} \subset \Phi_{\tilde{g}}(\Gamma \times [0, r_0]), \quad \tilde{g} \in \mathcal{G},$$

where $r_0 > 0$ is fixed.

We begin by showing the following consequence of the implicit function theorem.

Lemma 9. *Let $U \subset \mathbb{R}^n$ be open and let $\Phi_0 : \bar{U} \rightarrow \mathbb{R}^n$ be continuously differentiable. Let $p_0 \in U$ and suppose that the derivative $D\Phi_0$ is invertible at p_0 . Then there are neighbourhoods $W \subset \mathbb{R}^n$ of $\Phi_0(p_0)$ and $\mathcal{U} \subset C^1(\bar{U})$ of Φ_0 such that*

$$\|\Phi^{-1} - \Phi_0^{-1}\|_{C^0(\bar{W})} \leq C \|\Phi - \Phi_0\|_{C^1(\bar{U})}, \quad \Phi \in \mathcal{U}.$$

Proof. Define the map

$$F : C^1(\bar{U}) \times \mathbb{R}^n \times \mathbb{R}^n \rightarrow \mathbb{R}^n, \quad F(\Phi, q, p) = \Phi(p) - q.$$

Then F is continuously differentiable, and $D_p F(\Phi_0, p_0) = D\Phi_0(p_0)$. Thus the implicit function theorem, see e.g. [28, Th 6.2.1], implies that there are neighbourhoods $V, W' \subset \mathbb{R}^n$ of $p_0, \Phi_0(p_0)$ and $\mathcal{U}' \subset C^1(\bar{U})$ of Φ_0 , and a continuously differentiable map $H : \mathcal{U}' \times W' \rightarrow V$ such that $F(\Phi, q, H(\Phi, q)) = 0$. But this means that $H(\Phi, \cdot) = \Phi^{-1}$ in W' . Choose a neighbourhood W of $\Phi_0(p_0)$ such that $\bar{W} \subset W'$ and that \bar{W} is compact. As H is continuously differentiable, there is a neighbourhood $\mathcal{U} \subset \mathcal{U}'$ of Φ_0 such that

$$|H(\Phi, q) - H(\Phi_0, q)| \leq 2 \max_{q \in \bar{W}} \|D_\Phi H(\Phi_0, q)\|_{C^1(\bar{U}) \rightarrow \mathbb{R}^n} \|\Phi - \Phi_0\|_{C^1(\bar{U})}, \quad \Phi \in \mathcal{U}.$$

We have the following stability result in the isotropic case.

Theorem 10. *Consider a family \mathcal{G} of smooth isotropic metrics $\tilde{g} = \tilde{c}^{-2} dx^2$ satisfying (21). Let $c^{-2} dx^2 \in \mathcal{G}$ and suppose that*

$$(22) \quad \|\tilde{c} - c\|_{C^2(M)} \leq \epsilon, \quad \tilde{c}^{-2} dx^2 \in \mathcal{G}.$$

Then for small enough $\epsilon > 0$, there is $C > 0$ such that

$$\|\tilde{c}^2 - c^2\|_{C(\Omega)} \leq C \|H_{\tilde{c}} - H_c\|_{C^1(M) \rightarrow C^1(\Gamma \times [0, r_0])}.$$

Proof. We write $\Sigma = \Gamma \times (0, r_0)$, $\tilde{g} = \tilde{c}^{-2} dx^2$ and $g = c^{-2} dx^2$. Then (16) implies that

$$\|\Phi_{\tilde{g}} - \Phi_g\|_{C^1(\Sigma)} \leq C \|H_{\tilde{c}} - H_c\|_{C^1(M) \rightarrow C^1(\Sigma)}.$$

Moreover, again by (16),

$$\|\tilde{c}^2 \circ \Phi_{\tilde{g}} - c^2 \circ \Phi_g\|_{C^0(\Sigma)} \leq C \|H_{\tilde{c}} - H_c\|_{C^1(M) \rightarrow C^1(\Sigma)}.$$

This together with

$$\begin{aligned} \|\tilde{c}^2 - c^2\|_{C^0(\Omega)} &\leq \left\| \tilde{c}^2 \circ \Phi_{\tilde{g}} \circ \Phi_{\tilde{g}}^{-1} - c^2 \circ \Phi_g \circ \Phi_g^{-1} \right\|_{C^0(\Omega)} \\ &\quad + \left\| c^2 \circ \Phi_g \circ \Phi_g^{-1} - c^2 \circ \Phi_{\tilde{g}} \circ \Phi_{\tilde{g}}^{-1} \right\|_{C^0(\Omega)} \end{aligned}$$

implies that it is enough to study $\left\| \Phi_{\tilde{g}}^{-1} - \Phi_g^{-1} \right\|_{C^0(\Omega)}$.

Note that $(\tilde{g}, y, s) \mapsto \Phi_{\tilde{g}}(y, s)$ is continuously differentiable since it is obtained by solving the ordinary differential equation that gives the geodesics with respect to \tilde{g} . Indeed, this follows from [28, Th. 6.5.2] by considering the vector field F that generates the geodesic flow. In any local coordinates, $F(x, \xi, h) = (\xi, f(x, \xi, h), 0)$ where $f = (f^1, \dots, f^n)$, $f^j(x, \xi, h) = -\Gamma_{k\ell}^j(x, h)\xi^k\xi^\ell$, and $\Gamma_{k\ell}^j(x, h)$ are the Christoffel symbols of a metric tensor h at x , that is,

$$\Gamma_{k\ell}^j(x, h) = \frac{1}{2}h^{jm} \left(\frac{\partial h_{mk}}{\partial x^\ell} + \frac{\partial h_{m\ell}}{\partial x^k} - \frac{\partial h_{k\ell}}{\partial x^m} \right).$$

In particular, if ω is a neighbourhood of $p_0 \in \Sigma$ and $\bar{\omega} \subset \Sigma$, then the map $\tilde{c} \mapsto \Phi_{\tilde{g}}$ is continuous from $C^2(M)$ to $C^1(\bar{\omega})$. Thus, for small enough $\epsilon > 0$ in (22), we may apply Lemma 9 to obtain

$$\left\| \Phi_{\tilde{g}}^{-1} - \Phi_g^{-1} \right\|_{C^0(W)} \leq C \|\Phi_{\tilde{g}} - \Phi_g\|_{C^1(\Sigma)},$$

where W is a neighbourhood of $\Phi_g(p_0)$. As $\bar{\Omega}$ is compact, it can be covered by a finite number of sets like the above set W . Thus

$$\left\| \Phi_{\tilde{g}}^{-1} - \Phi_g^{-1} \right\|_{C^0(\Omega)} \leq C \|\Phi_{\tilde{g}} - \Phi_g\|_{C^1(\Sigma)} \leq C \|H_{\tilde{c}} - H_c\|_{C^1(M) \rightarrow C^1(\Sigma)}.$$

We now consider the anisotropic case, and describe a geometric condition on (M, g) that will yield stable recovery of g in the semi-geodesic coordinates of Γ from L_g in the set Ω . Specifically, we will assume that the following problem, which is the dual problem to (2),

$$(23) \quad \begin{aligned} \partial_t^2 w - \Delta_g w &= 0, & \text{in } (0, T) \times M, \\ w|_{x \in \partial M} &= 0 \\ w|_{t=T} = 0, \quad \partial_t w|_{t=T} &= \phi. \end{aligned}$$

is *stably observable* in the following sense.

Definition 11. *Let \mathcal{G} be a subset of smooth Riemannian metrics on M . Then, (23) is stably observable for Ω and \mathcal{G} from Γ in time $T > 0$ if there is a constant $C > 0$ such that for all $g \in \mathcal{G}$ and for all $\phi \in L^2(\Omega)$ the solutions $w = w^\phi = w^{\phi, g}$ of (23) uniformly satisfy*

$$(24) \quad \|\phi\|_{L^2(\Omega)} \leq C \left\| \partial_\nu w^\phi \right\|_{L^2((0, T) \times \Gamma)}.$$

A complete characterization of metrics exhibiting stable observability is not presently known, however, it is known that stable observability holds under suitable convexity conditions. Indeed, if (M, g) admits a strictly convex function ℓ without critical points, and satisfies

$$\{x \in \partial M; (\nabla \ell(x), \nu)_g \geq 0\} \subset \Gamma,$$

then there is a neighbourhood \mathcal{G} of g and $T > 0$ such that (23) is stably observable for M and \mathcal{G} from Γ in time $T > 0$, see [30]. Note that this result gives stable observability over the complete manifold M but we will need it only over the set Ω .

Stable observability in the case of Neumann boundary condition is poorly understood presently. For instance, stable observability can not be easily derived from an estimate like [33, Th 3], the reason being that the H^1 -norm of the Dirichlet trace of a solution to the wave equation is not bounded by the L^2 -norm of the Neumann trace, while the opposite is true [33, Th. 4]. See also [38] for a detailed discussion. For this reason we restrict our attention to the case of Dirichlet boundary condition.

We use the notation

$$W_g f(x) = u^f(T, \cdot)|_{\Omega}, \quad f \in L^2([0, T] \times \Gamma).$$

The stable observability (24) says that W_g^* is injective, and by duality, it implies that $W_g : L^2([0, T] \times \Gamma) \rightarrow L^2(\Omega)$ is surjective (see [2]). In this case (2) is said to be exactly controllable on Ω , and in particular, for any $\phi \in L^2(\Omega)$ the control problem $W_g f = \phi$ has the minimum norm solution $f = W_g^\dagger \phi$ given by the pseudoinverse of W_g .

Theorem 12. *Consider a family \mathcal{G} of metrics \tilde{g} satisfying (21) and suppose that (23) is stably observable for Ω and \mathcal{G} from Γ in time $T > 0$. Let $g \in \mathcal{G}$ and suppose that*

$$(25) \quad \|\tilde{g} - g\|_{C^2(M)} \leq \epsilon, \quad \tilde{g} \in \mathcal{G}.$$

Then for small enough $\epsilon > 0$, there is $C > 0$ such that

$$\|\Psi^* \tilde{g} - g\|_{H^{-2}(\Omega)} \leq C \|L_{\tilde{g}} - L_g\|_*, \quad \tilde{g} \in \mathcal{G},$$

where $\Psi^* = (\Phi_g^*)^{-1} \Phi_{\tilde{g}}^*$ and

$$\|L_g\|_* = \|L_g\|_{L^2((0, T) \times \Gamma) \rightarrow L^2(\Gamma \times (0, \epsilon))} + \|L_g \circ \partial_t^2\|_{L^2((0, T) \times \Gamma) \rightarrow H^{-2}(\Gamma \times (0, \epsilon))}.$$

Proof. We use again the notation $\Sigma = \Gamma \times (0, r_0)$ and write also $\Sigma_T = \Gamma \times (0, T)$. Let $p \in \Sigma$, and denote by (x^1, \dots, x^n) the coordinates on Σ corresponding to local semi-geodesic coordinates (y, r) . Let $j, k = 1, \dots, n$ and let $\omega \subset \Sigma$ be a neighbourhood of p . Choose $\phi_\ell \in C_0^\infty(\Sigma)$, $\ell = 1, 2, 3$, as in (18). Note that solving (19) and taking the limit $\alpha \rightarrow 0$ is equivalent with computing $L^\dagger \phi^\ell$ see e.g. [17, Th. 5.2].

Analogously to (20), writing the change to local coordinates explicitly, it holds that

$$(\Phi_g^*)^{jk}(x) = \frac{1}{2}(L_g \partial_t^2 h_1(x) - x^k L_g \partial_t^2 h_2(x) - x^j L_g \partial_t^2 h_3(x)),$$

where $h_\ell = L_g^\dagger \phi_\ell$, $\ell = 1, 2, 3$. It will be enough to bound

$$\left\| L_{\tilde{g}} \partial_t^2 L_{\tilde{g}}^\dagger \phi_\ell - L_g \partial_t^2 L_g^\dagger \phi_\ell \right\|_{H^{-2}(\omega)}, \quad \ell = 1, 2, 3,$$

in terms of the difference $L_{\tilde{g}} - L_g$. We have

$$\begin{aligned} & \left\| L_{\tilde{g}} \partial_t^2 L_{\tilde{g}}^\dagger \phi_\ell - L_g \partial_t^2 L_g^\dagger \phi_\ell \right\|_{H^{-2}(\omega)} \\ & \leq \left\| L_{\tilde{g}} \partial_t^2 L_{\tilde{g}}^\dagger \phi_\ell - L_g \partial_t^2 L_{\tilde{g}}^\dagger \phi_\ell \right\|_{H^{-2}(\omega)} + \left\| L_g \partial_t^2 L_{\tilde{g}}^\dagger \phi_\ell - L_g \partial_t^2 L_g^\dagger \phi_\ell \right\|_{H^{-2}(\omega)} \\ & \leq \left\| (L_{\tilde{g}} - L_g) \circ \partial_t^2 \right\|_{L^2(\Sigma_T) \rightarrow H^{-2}(\Sigma)} \left\| L_{\tilde{g}}^\dagger \right\|_{L^2(\Sigma) \rightarrow L^2(\Sigma_T)} \|\phi_\ell\|_{L^2(\Sigma)} \\ & \quad + \left\| L_g \circ \partial_t^2 \right\|_{L^2(\Sigma_T) \rightarrow H^{-2}(\Sigma)} \left\| L_{\tilde{g}}^\dagger - L_g^\dagger \right\|_{L^2(\Sigma) \rightarrow L^2(\Sigma_T)} \|\phi_\ell\|_{L^2(\Sigma)}. \end{aligned}$$

We omit writing subscripts in operator norms below as their meaning should be clear from the context. Pseudoinversion is continuous in the sense that

$$\left\| L_{\tilde{g}}^\dagger - L_g^\dagger \right\| \leq 3 \max \left(\left\| L_{\tilde{g}}^\dagger \right\|, \left\| L_g^\dagger \right\| \right) \|L_{\tilde{g}} - L_g\|,$$

see e.g. [19]. It remains to show that $\left\| L_{\tilde{g}}^\dagger \right\|$ is uniformly bounded for \tilde{g} satisfying (25). Note that $L_{\tilde{g}} = \Phi_{\tilde{g}}^* W_{\tilde{g}}$ and recall that (24) implies $\left\| (W_{\tilde{g}}^*)^\dagger \right\| \leq C$, which again implies that $\left\| W_{\tilde{g}}^\dagger \right\| \leq C$. Here the constant C is uniform for $\tilde{g} \in \mathcal{G}$. Moreover Lemma 9 implies that, for small enough $\epsilon > 0$ in (25), we have $\left\| (\Phi_{\tilde{g}}^*)^{-1} \right\| \leq C$. To summarize, there is uniform constant C for \tilde{g} satisfying (25) such that

$$\left\| \Phi_{\tilde{g}}^* \tilde{g} - \Phi_g^* g \right\|_{H^{-2}(\omega)} \leq C \|L_{\tilde{g}} - L_g\|_* \|\phi_\ell\|_{L^2(\Sigma)}.$$

The claim follows by using a partition of unity. Note that the functions ϕ_ℓ can be chosen so that they are uniformly bounded in L^2 when ω is varied. \blacksquare

6. Computational experiment. In this section, we provide a computational experiment to demonstrate our approach to recovering an isotropic wave speed from the N-to-D map. We conduct our computational experiment in the case where M is a domain in \mathbb{R}^2 , however, we stress that our approach generalizes to any $n \geq 2$.

6.1. Forward modelling and control solutions. For our computational experiment, we consider waves propagating in the lower half-space $M = \mathbb{R} \times (-\infty, 0]$ with respect to the following wave speed:

$$(26) \quad c(x_1, x_2) = 1 + \frac{1}{2}x_2 - \frac{1}{2} \exp(-4(x_1^2 + (x_2 - 0.375)^2)).$$

See Figure 2. Waves are simulated and recorded at the boundary for time $2T$, where $T = 1.0$. Sources are placed inside the accessible set $\Gamma = [-\ell_s, \ell_s] \times \{0\}$, where $\ell_s = 3.0$, and receiver measurements are made in the set $\mathcal{R} = [-\ell_r, \ell_r] \times \{0\}$, where $\ell_r = 4.5$.

For sources, we use a collection of Gaussian functions spanning a subspace of $L^2([0, T] \times \Gamma)$. Specifically, we consider sources of the form

$$\varphi_{i,j}(t, x) = C \exp(-a((t - t_{s,i})^2 + (x - x_{s,j})^2)).$$

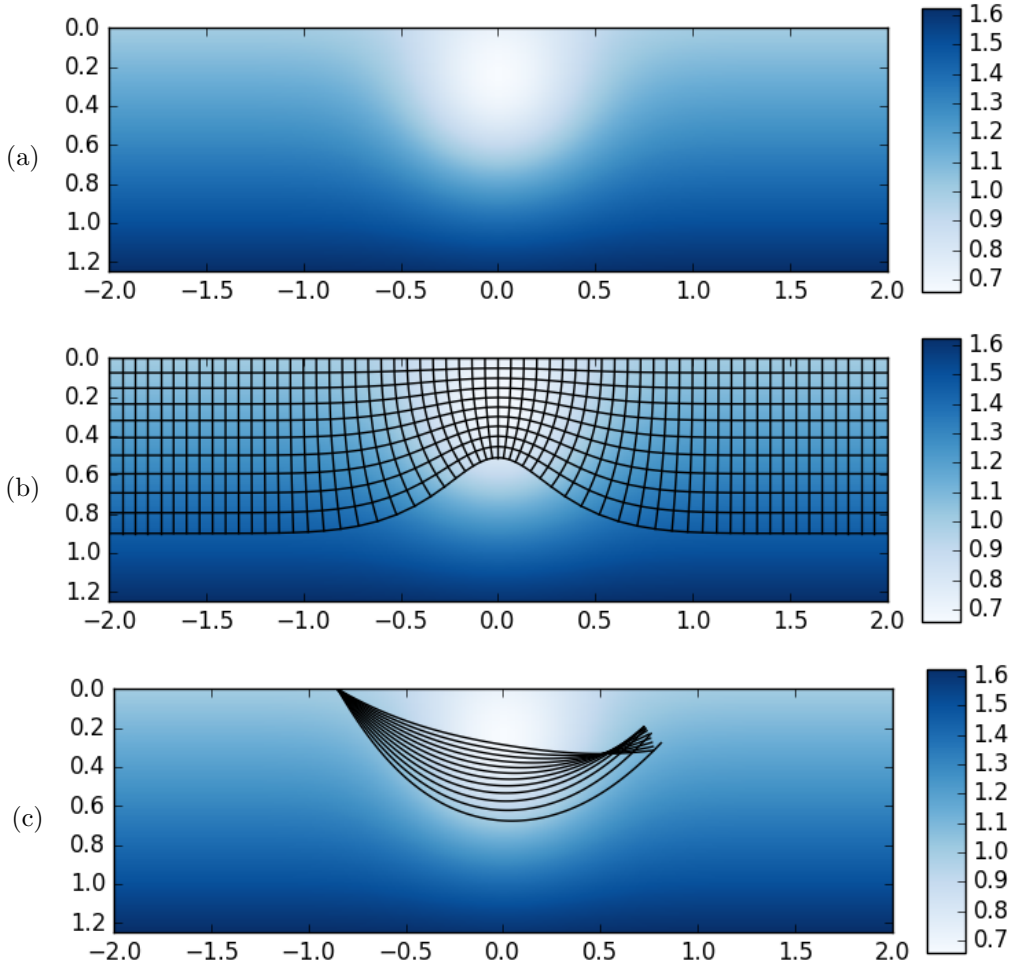


Figure 2: (a) True wave speed c . (b) Semi-Geodesic coordinate grid associated with c . (c) Some example ray paths with non-orthogonal intersection to ∂M .

Here, the pairs $(t_{s,i}, x_{s,j})$ are chosen to form a uniformly spaced grid in $[0.025, 0.975] \times [-\ell_s, \ell_s]$ with spacing $\Delta t_s = \Delta x_s = 0.025$. In total, we consider $N_{t,s} = 39$ source times $t_{s,i}$ and $N_{x,s} = 241$ source locations $x_{s,j}$. The constant a , controlling the width of the basis functions in space and time, is taken as $a = 1381.6$, and the constant C is chosen to normalize the functions $\varphi_{i,j}$ in $L^2([0, T] \times \Gamma)$.

Wave propagation is simulated using a continuous Galerkin finite element method with Newmark time-stepping. Waves are simulated for $t \in [-t_0, 2T]$, where $t_0 = 0.1$, although N-to-D measurements are only recorded in $[0, 2T]$. The short buffer interval, $[-t_0, 0]$, is added to the simulation interval in order to avoid numerical dispersion from non-vanishing sources at $t = 0$. The sources are extended to Receiver measurements are simulated by recording the Dirichlet trace $\Lambda_{\Gamma, \mathcal{R}}^{2T} \varphi_{i,j}$ at uniformly spaced points $x_{s,r} \in [\ell_r, \ell_r]$ with spatial separation

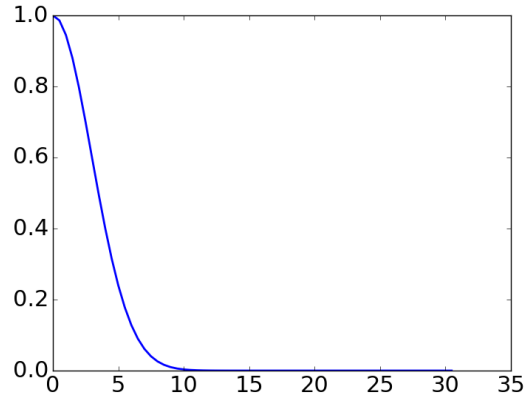


Figure 3: Power spectrum of $\varphi_{ij}(\cdot, x_{s,i})$, measured in Hz. We have rescaled the power spectrum so that it has a maximum value of 1.

$\Delta x_r = 0.0125$ at uniformly spaced times $t_{s,r} \in [0, 2T]$ with temporal spacing $\Delta t_r = 0.0025$. Note that our receiver measurements are sampled more densely in both space and time than our source applications. In particular, $\Delta x_r = 0.5\Delta x_s$ and $\Delta t_r = 0.1\Delta t_s$. In total, we take $N_{t,r} = 801$ receiver measurements at each of the $N_{x,r} = 721$ receiver positions.

We briefly comment on the physical scales associated with the computational experiment. In the units above, the wave speed is approximately 1 at the surface. If we take this to represent a wave speed of approximately 2000m/s and suppose that the receiver spacing corresponds to $\Delta x_r = 12.5$ m, then in the same units $\Delta t_r = .00125$ s. In addition, we have that $\ell_s = 4.5$ km and $T = 1.0$ s, which implies that receivers are placed within a 9.0km region and traces are recorded for a total of 2.0s. In Fig. 3 we plot the power spectrum for one of the sources at a fixed source location, to give a sense of the frequencies involved. Note that the source mostly consists of frequencies below 15Hz.

In this computational experiment, we have used sources that have a significant frequency component at 0 Hz. Such low frequency contributions are not representative of physical source wavelets, so it may be of interest to note that the data we have used can be synthesized from sources which lack 0 Hz components. In particular, these data used can be synthesized by post-processing data from sources that are products of Gaussians in space and Ricker wavelets in time. We note that Ricker wavelets are the second derivatives of Gaussian functions, and that they are zero-mean sources (hence they vanish at 0 Hz) that are frequently used as sources when simulating synthetic seismic data. To demonstrate the claim, we first show that $u^{If} = I(u^f)$, where I denotes the integral $Ih(t, \cdot) := \int_0^t h(s, \cdot) ds$. To see this, we first observe

that,

$$\begin{aligned}\partial_t^2(Iu^f) &= \partial_t^2\left(\int_0^t u^f(s, \cdot) ds\right) = \partial_t u^f(t, \cdot) = \int_0^t \partial_t^2 u^f(s, \cdot) ds - \partial_t u^f(0, \cdot) \\ &= \int_0^t c^2(x)\Delta u^f(s, \cdot) ds = c^2(x)\Delta(Iu^f).\end{aligned}$$

Here, we have used the fact that $\partial_t u^f(0, \cdot) = 0$ and $(\partial_t^2 - c^2(x)\Delta)u^f = 0$ since u^f solves (1). Likewise, because u^f solves (1), it follows that $\partial_n(Iu^f) = I(\partial_n u^f) = If$ and that $\partial_t Iu^f(0, \cdot) = u^f(0, \cdot) = 0$. Since $Iu^f(0, \cdot) = \int_0^0 u^f(s, \cdot) ds = 0$, we see that Iu^f satisfies:

$$\begin{aligned}\partial_t^2 w - c^2(x)\Delta w &= 0, & \text{in } (0, \infty) \times M, \\ \partial_{\vec{n}} w|_{x \in \partial M} &= If, \\ w|_{t=0} = \partial_t w|_{t=0} &= 0,\end{aligned}$$

thus Iu^f solves (1) with Neumann source If . Since solutions to (1) are unique, we see that $Iu^f = u^{If}$, as claimed. An immediate consequence is that,

$$I\Lambda_{\Gamma, \mathcal{R}}^{2T} f = Iu^f|_{\mathcal{R}} = u^{If}|_{\mathcal{R}} = \Lambda_{\Gamma, \mathcal{R}}^{2T} If.$$

Thus, $\Lambda_{\Gamma, \mathcal{R}}^{2T} I^j f = I^j \Lambda_{\Gamma, \mathcal{R}}^{2T} f$ for $j \in \mathbb{N}$. Next, we let $\psi_{i,j} = \partial_t^2 \varphi_{i,j}$, and note that $\psi_{i,j}$ is a product of a Ricker wavelet in time (since it is the second time derivative of a Gaussian function) and a Gaussian in space. We then observe that,

$$\varphi_{i,j}(t, x) = \varphi_{i,j}(0, x) + t\partial_t \varphi_{i,j}(0, x) + I^2 \psi_{i,j}(0, x).$$

Under the parameter choices for $\varphi_{i,j}$, the first two terms are considerably smaller than the third for $i \geq 4$, since 0 belongs to the tail of the Gaussian $\varphi_{i,j}$. For $i \leq 3$, the same comment holds if we replace $t = 0$ by the buffer interval start-time, $t = -t_0$ (likewise, we would need to replace $t = 0$ by $t = -t_0$ when applying I). In either event, $\varphi_{i,j} \approx I^2 \psi_{i,j}$, and $\Lambda_{\Gamma, \mathcal{R}}^{2T} \varphi_{i,j} \approx I^2(\Lambda_{\Gamma, \mathcal{R}}^{2T} \psi_{i,j})$. For our particular set-up, the N-to-D data agreed to within an error of about 1 part in 10^{-4} . To recapitulate, the data that we have used could be approximately synthesized by first using the (more) realistic sources $\psi_{i,j}$ to simulate the data $\Lambda_{\Gamma, \mathcal{R}}^{2T} \psi_{i,j}$, and then post-processing these data by integrating them twice in time.

We introduce some notation, which we will use when discussing our discretization of the connecting operator and control problems. First, let $f \in L^2([0, T] \times \Gamma)$. We use the notation $[f]$ to denote the vector of inner-products with entries $[f]_i = \langle f, \varphi_i \rangle_{L^2([0, T] \times \Gamma)}$. In addition, we let \hat{f} denote the coefficient-vector for the projection of f onto $\text{span}\{\varphi_i\}$. Let A be an operator on $L^2([0, T] \times \Gamma)$. We will use the notation $[A]$ to denote the matrix of inner-products $[A]_{ij} = \langle A\varphi_i, \varphi_j \rangle_{L^2([0, T] \times \Gamma)}$. We approximate all such integrals by successively applying the trapezoidal rule in each dimension.

After the N-to-D data has been generated, we use the data $\Lambda_{\Gamma}^{2T} \varphi_{i,j}$ to discretize the connecting operator. We accomplish this using a minor modification of the procedure outlined in [16]. In particular, we discretize the connecting operator by computing a discrete approxi-

mation to (6):

$$[K] = [J\Lambda_\Gamma^{2T}] - [R\Lambda_\Gamma^T]G^{-1}[RJ].$$

Here, G^{-1} denotes the inverse of the Gram matrix $G_{ij} = \langle \varphi_i, \varphi_j \rangle_{L^2([0,T] \times \Gamma)}$.

Next, we describe our implementation of Lemma 2. Let $y \in \Gamma$, $s \in [0, T]$ and $h \in [0, T - s]$. To obtain the control $\psi_{\alpha,h}$ associated with $\text{cap}_\Gamma(y, s, h)$, we solve two discrete versions of the boundary control problem (7). Specifically, for $\tau_1 = s1_\Gamma$ and $\tau_2 = \tau_y^{s+h} \vee s1_\Gamma$, we solve the discretized control problems:

$$(27) \quad ([K_{\tau_k}] + \alpha)\hat{f} = [b_{\tau_k}].$$

This yields coefficient vectors $\hat{f}_{\alpha,k}$, for $k = 1, 2$ associated with the approximate control solutions. Here, we use the notation $[K_{\tau_k}]$ to denote a matrix that deviates slightly from the definition given above. In particular, we obtain $[K_{\tau_k}]$ from $[K]$ by masking rows and columns corresponding to basis functions $\varphi_{i,j}$ localized near $(t_{s,i}, x_{s,j}) \notin S_{\tau_k}$. This gives an approximation to the matrix for $K_{\tau_k} = P_{\tau_k} K P_{\tau_k}$, which we have observed performs well for our particular basis. The right-hand side vector $[b_{\tau_k}]$ is a discrete approximation to $P_{\tau_k} b$ and we obtain it by first computing the vector of inner-products $[b]_l = \langle b, \varphi_l \rangle_{L^2([0,T] \times \Gamma)}$, and then masking the entries of $[b]$ using the same strategy that we use to compute $[K_{\tau_k}]$. We solve the control problems (27) using Matlab's back-slash function. After computing the solutions $\hat{f}_{\alpha,k}$, we then compute $\psi_{h,\alpha} = f_{\alpha,2} - f_{\alpha,1}$.

In the inversion step, we use the boundary data to approximate harmonic functions in semi-geodesic coordinates in the interior of M . To describe this step, let ϕ be a harmonic function in M . Fix y, s , and h , and let $\psi_{\alpha,h}$ denote the control constructed as in the previous paragraph. We define:

$$(28) \quad H_{c,h}\phi(y, s) := \frac{B(\psi_{h,\alpha}, \phi)}{B(\psi_{h,\alpha}, 1)},$$

and we calculate the right hand side directly using (13). Note that this expression coincides with an approximation to the leading term in the right-hand side of (11), so for small h and α , $H_{c,h}\phi(y, s)$ will approximate $H_c\phi(y, s)$. However, we recall that (11) is only accurate to $\mathcal{O}(h^{1/2})$, and in practice we found that (28) tends to be closer to $H_c\phi(y, s + h/2) = \phi(x(y, s + h/2))$. This is not unexpected, since (28) approximates $H_c\phi(y, s)$ by approximating the average of ϕ over $B_h = \text{cap}_\Gamma(y, s, h)$, and the point $x(y, s)$ belongs to the topological boundary of B_h , whereas $x(y, s + h/2)$ belongs to the interior of B_h . Consequently, we will compare $H_{c,h}\phi(y, s)$ to $H_c\phi(y, s + h/2)$ below.

6.2. Inverting for the wave speed. Our approach to reconstruct the wave speed c consists of two steps. In the first step, we implement Proposition 6 to compute an approximation to the coordinate transform Φ_c on a grid of points $(y_i, s_j) \in \Gamma \times [0, T]$. The second step is to differentiate the approximate coordinate transform in the s -direction and to apply (16) to compute the wave speed at the estimated points.

To approximate the coordinate transform Φ_c , we first fix a small wave cap height $h > 0$, which we use at every grid point. The wave cap height controls the spatial extent of the

waves $u^{\psi_{h,\alpha}}(T, \cdot)$ in the interior of M . Because the vertical resolution of our basis is controlled by the separation between sources in time, we choose h to be an integral multiple of Δt_s , and in particular, we take $h = 2\Delta t_s$. Likewise, we choose the grid-points (y_i, s_j) to coincide with the source centers for a subset of our basis functions. Specifically, we take $y_i = x_{s,i}$ and $s_j = t_{s,j}$ for the source locations $x_{s,i} \in [-1.5, 1.5]$ and times $t_{s,j} \in [0.05, 0.65]$. In total, the reconstruction grid contains $N_{x,g} = 121$ horizontal positions, and $N_{t,g} = 27$ vertical positions. Then, for each grid point (y_i, s_j) we solve (27) for $k = 1, 2$, and obtain the source $\psi_{i,j} = \psi_{\alpha,h}$ for the point (y_i, s_j) . Since the Cartesian coordinate functions x^1 and x^2 are both harmonic, we then apply (28) to both functions at each grid point, and define

$$(29) \quad \Phi_{c,h}(y_i, s_j) := (H_{c,h}x^1(y_i, s_j), H_{c,h}x^2(y_i, s_j)).$$

This yields the desired approximate coordinate transform. We plot the estimated coordinates in Figure 4a and compare the estimated transform $\Phi_{c,h}(y_i, s_j)$ to the points $\Phi(y_i, s_j + h/2)$ in Figure 4b.

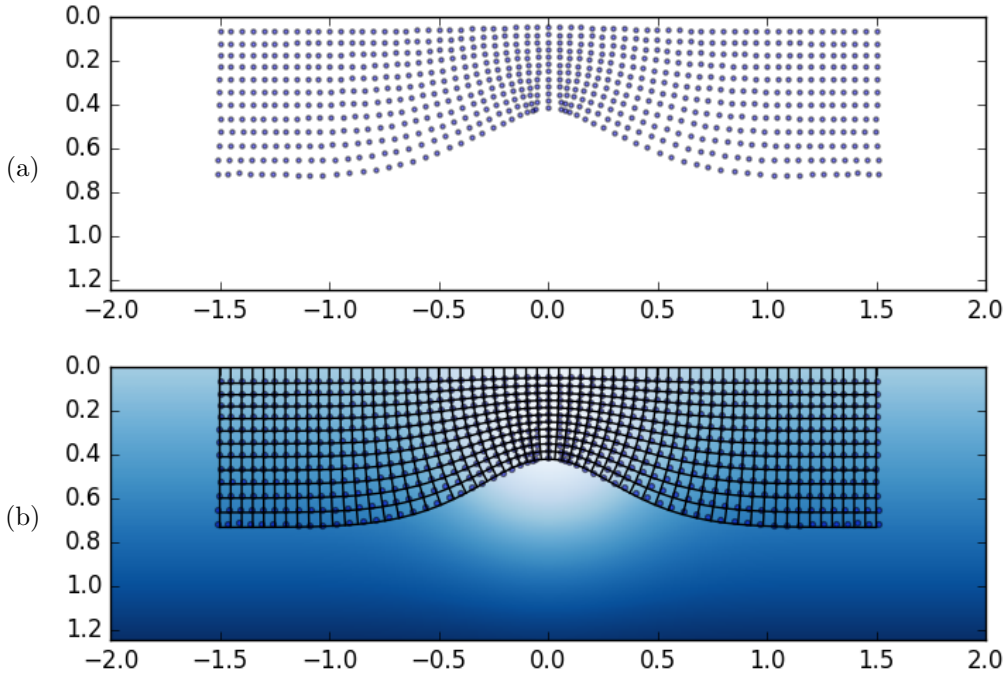


Figure 4: (a) The estimated coordinate transform. We have only plotted points for half of the y_i and s_j . (b) Estimated points $\Phi_{c,h}(y_i, s_j)$ (purple dots) compared to the semi-geodesic coordinate grid $\Phi_c(y_i, s_j + h/2)$ (black lines) and wave speed.

The last step is to approximate the wave speed. To accomplish this, we first recall that $c(\Phi_c(y, s))^2 = |\partial_s \Phi_c(y, s)|_e^2$. Thus, for each base point y_i , we fit a smoothing spline to each of the reconstructed coordinates in the s -direction, that is, we fit a smoothing spline to the data sets $\{H_{c,h}x^k(y_i, s_j) : j = 1, \dots, N_{t,g}\}$ for $k = 1, 2$ for each $i = 1, \dots, N_{x,g}$. We

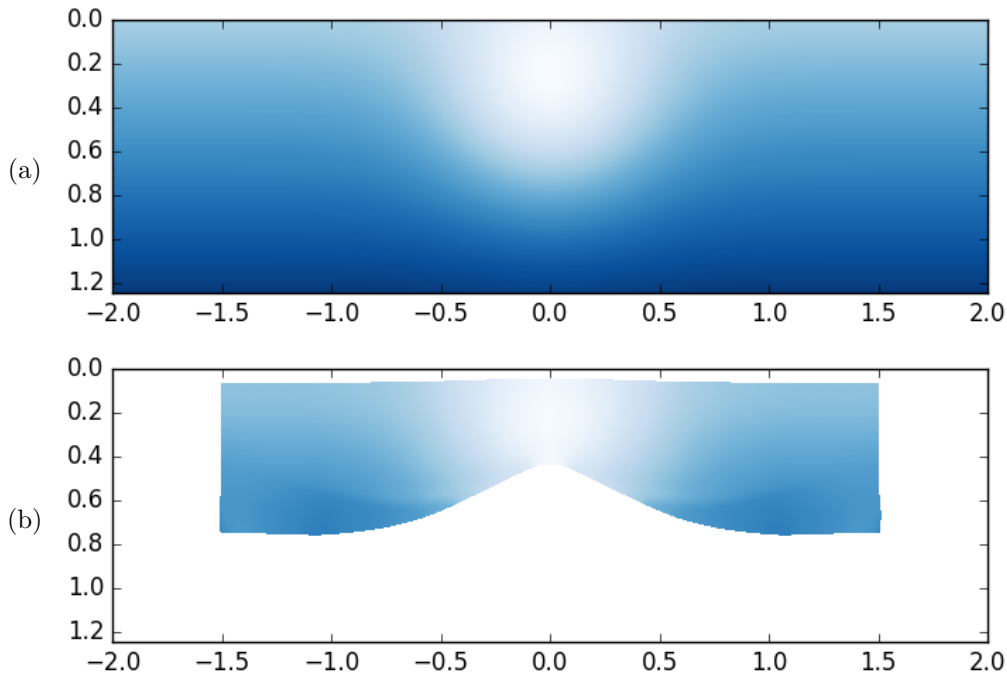


Figure 5: (a) True wave speed c . (b) Reconstructed wave speed, plotted at the estimated coordinates given by $\Phi_{c,h}$.

then differentiate the resulting splines at s_j , for $j = 1, \dots, N_{t,g}$ to approximate the derivatives $\partial_s H_{c,h} x^k(y_i, s_j)$, at each grid point. Finally, we estimate $c(\Phi_{c,h}(y_i, s_j))$ by computing $|(\partial_s H_{c,h} x^1(y_i, s_j), \partial_s H_{c,h} x^2(y_i, s_j))|_e$. We plot the results of this process in Figure 5, along with the true wave speed for comparison. We also compare the reconstructed wave speed against the true wave speed in Figure 6 along coordinate slices.

Inspecting the bottom row of Figure 6, we see that the reconstruction is generally good at the estimated points. In particular, the reconstruction quality generally decreases as s_j increases, which is expected, since the points $\Phi_{c,h}(y_i, s_j)$ with large s_j correspond to the points which are furthest from the set Γ . Hence the N-to-D data contains a shorter window of signal returns from these points, and thus less information about the wave speed there.

REFERENCES

- [1] G. BAL, *Hybrid inverse problems and internal functionals*, in *Inverse problems and applications: inside out. II*, vol. 60 of *Math. Sci. Res. Inst. Publ.*, Cambridge Univ. Press, Cambridge, 2013, pp. 325–368.
- [2] C. BARDOS AND M. BELISHEV, *The wave shaping problem*, in *Partial Differential Equations and Functional Analysis*, J. Cea, D. Chenais, G. Geymonat, and J. Lions, eds., vol. 22 of *Progress in Nonlinear Differential Equations and Their Applications*, Birkhuser Boston, 1996, pp. 41–59, https://doi.org/10.1007/978-1-4612-2436-5_4.
- [3] L. BAUDOIN, M. DE BUHAN, AND S. ERVEDOZA, *Convergent algorithm based on carleman estimates for the recovery of a potential in the wave equation*, Preprint arXiv:1610.07400, (2016), <https://arxiv.org/abs/1610.07400>.

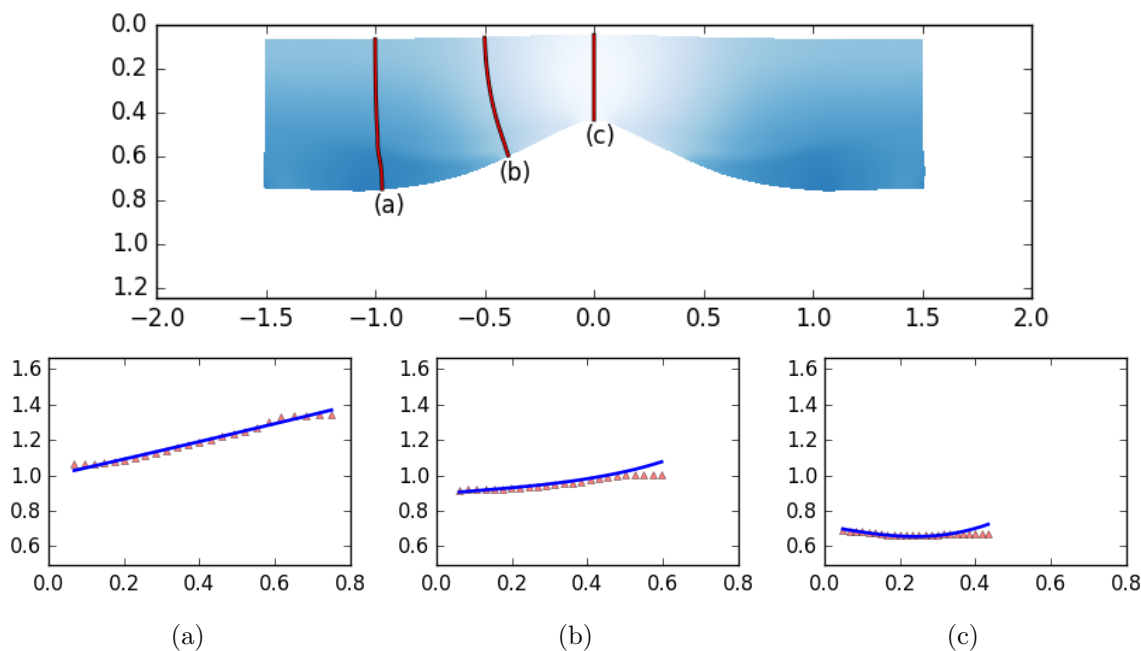


Figure 6: Top: Reconstructed wave speed with three approximated geodesics. Bottom row: true wave speed (blue curve) and reconstructed wave speed (red triangles) evaluated at the estimated coordinates for each of the indicated geodesics. The x -axis denotes the x^2 -coordinate (depth) along the approximated geodesic.

[org/abs/1610.07400](https://arxiv.org/abs/1610.07400).

- [4] L. BEILINA AND M. V. KLIBANOV, *A globally convergent numerical method for a coefficient inverse problem*, SIAM J. Sci. Comput., 31 (2008), pp. 478–509, <https://doi.org/10.1137/070711414>.
- [5] L. BEILINA AND M. V. KLIBANOV, *Approximate global convergence and adaptivity for coefficient inverse problems*, Springer, 2012.
- [6] M. BELISHEV AND Y. Y. GOTLIB, *Dynamical variant of the BC-method: theory and numerical testing.*, Journal of Inverse & Ill-Posed Problems, 7 (1999), p. 221.
- [7] M. I. BELISHEV, *An approach to multidimensional inverse problems for the wave equation*, Dokl. Akad. Nauk SSSR, 297 (1987), pp. 524–527.
- [8] M. I. BELISHEV, *Recent progress in the boundary control method*, Inverse Problems, 23 (2007), pp. R1–R67, <https://doi.org/10.1088/0266-5611/23/5/R01>.
- [9] M. I. BELISHEV, I. B. IVANOV, I. V. KUBYSHKIN, AND V. S. SEMENOV, *Numerical testing in determination of sound speed from a part of boundary by the BC-method*, J. Inverse Ill-Posed Probl., 24 (2016), pp. 159–180, <https://doi.org/10.1515/jiip-2015-0052>.
- [10] K. BINGHAM, Y. KURYLEV, M. LASSAS, AND S. SILTANEN, *Iterative time-reversal control for inverse problems*, Inverse Probl. Imaging, 2 (2008), pp. 63–81, <https://doi.org/10.3934/ipi.2008.2.63>.
- [11] R. BOSI, Y. KURYLEV, AND M. LASSAS, *Stability of the unique continuation for the wave operator via Tataru inequality and applications*, J. Differential Equations, 260 (2016), pp. 6451–6492, <https://doi.org/10.1016/j.jde.2015.12.043>.
- [12] R. BOSI, Y. KURYLEV, AND M. LASSAS, *Reconstruction and stability in gel'fand's inverse interior spectral problem*, Preprint arXiv:1702.07937, (2017), <https://arxiv.org/abs/1702.07937>.
- [13] A. L. BUKHGEĬ M AND M. V. KLIBANOV, *Uniqueness in the large of a class of multidimensional inverse*

- problems, Dokl. Akad. Nauk SSSR, 260 (1981), pp. 269–272.
- [14] M. DE HOOP, S. HOLMAN, E. IVERSEN, M. LASSAS, AND B. URSIN, *Reconstruction of a conformally Euclidean metric from local boundary diffraction travel times*, SIAM Journal on Mathematical Analysis, 46 (2014), pp. 3705–3726, <https://doi.org/10.1137/130931291>.
- [15] M. V. DE HOOP, P. KEPLEY, AND L. OKSANEN, *An exact redatuming procedure for the inverse boundary value problem for the wave equation*, Submitted. Preprint arXiv:1612.02383, (2016), <https://arxiv.org/abs/1612.02383>.
- [16] M. V. DE HOOP, P. KEPLEY, AND L. OKSANEN, *On the construction of virtual interior point source travel time distances from the hyperbolic neumann-to-dirichlet map*, SIAM Journal on Applied Mathematics, 76 (2016), pp. 805–825, <https://doi.org/10.1137/15M1033010>.
- [17] H. ENGL, H., G. NEUBAUER, AND M. HANKE, *Regularization of Inverse Problems*, vol. 375 of Mathematics and Its Applications, Kluwer Academic Publishers-Plenum Publishers, 1996.
- [18] G. ESKIN, *Inverse problems for general second order hyperbolic equations with time-dependent coefficients*, Preprint arXiv:1503.00825, (2015), <https://arxiv.org/abs/1503.00825>.
- [19] S. IZUMINO, *Convergence of generalized inverses and spline projectors*, Journal of Approximation Theory, 38 (1983), pp. 269–278, [https://doi.org/10.1016/0021-9045\(83\)90133-8](https://doi.org/10.1016/0021-9045(83)90133-8).
- [20] S. I. KABANIKHIN, A. D. SATYBAEV, AND M. A. SHISHLENIN, *Direct methods of solving multidimensional inverse hyperbolic problems*, Inverse and Ill-posed Problems Series, VSP, Utrecht, 2005.
- [21] A. KATCHALOV, Y. KURYLEV, AND M. LASSAS, *Inverse boundary spectral problems*, vol. 123 of Monographs and Surveys in Pure and Applied Mathematics, Chapman & Hall/CRC, Boca Raton, FL, 2001, <https://doi.org/10.1201/9781420036220>.
- [22] A. KATSUDA, Y. KURYLEV, AND M. LASSAS, *Stability of boundary distance representation and reconstruction of Riemannian manifolds*, Inverse Problems and Imaging, 1 (2007), pp. 135–157, <https://doi.org/10.3934/ipi.2007.1.135>.
- [23] A. KIRSCH, *An Introduction to the Mathematical Theory of Inverse Problems*, Springer, New York, 2011, <https://doi.org/10.1007/978-1-4419-8474-6>.
- [24] M. V. KLIBANOV, A. E. KOLESOV, L. NGUYEN, AND A. SULLIVAN, *Globally strictly convex cost functional for a 1-d inverse medium scattering problem with experimental data*, Preprint arXiv:1703.08158, (2017), <https://arxiv.org/abs/1703.08158>.
- [25] M. V. KLIBANOV AND N. T. THÀNH, *Recovering dielectric constants of explosives via a globally strictly convex cost functional*, SIAM J. Appl. Math., 75 (2015), pp. 518–537, <https://doi.org/10.1137/140981198>.
- [26] Y. KURYLEV, *Multidimensional Gel'fand inverse problem and boundary distance map*, in Inverse Problems Related with Geometry, Proceedings of the Symposium at Tokyo Metropolitan University, 1997, pp. 1–15.
- [27] Y. KURYLEV, L. OKSANEN, AND G. P. PATERNAIN, *Inverse problems for the connection Laplacian*, Submitted. Preprint arXiv:1509.02645, <https://arxiv.org/abs/1509.02645>.
- [28] S. LANG, *Real Analysis*, Addison-Wesley Publishing Company, Reading, Massachusetts, 1983.
- [29] C. LAURENT AND M. LAUTAUD, *Quantitative unique continuation for operators with partially analytic coefficients. application to approximate control for waves*, Preprint arXiv:1506.04254, (2015), <https://arxiv.org/abs/1506.04254>.
- [30] S. LIU AND L. OKSANEN, *A Lipschitz stable reconstruction formula for the inverse problem for the wave equation*, Transactions of the American Mathematical Society, 368 (2016), pp. 319–335, <https://doi.org/10.1090/tran/6332>.
- [31] L. OKSANEN, *Solving an inverse problem for the wave equation by using a minimization algorithm and time-reversed measurements*, Inverse Problems and Imaging, 5 (2011), pp. 731–744, <https://doi.org/10.3934/ipi.2011.5.731>.
- [32] L. OKSANEN, *Solving an inverse obstacle problem for the wave equation by using the boundary control method*, Inverse Problems, 29 (2013), pp. 035004, 12, <https://doi.org/10.1088/0266-5611/29/3/035004>.
- [33] L. OKSANEN AND G. UHLMANN, *Photoacoustic and thermoacoustic tomography with an uncertain wave speed*, Math. Res. Lett., 21 (2014), pp. 1199–1214, <https://doi.org/10.4310/MRL.2014.v21.n5.a13>.
- [34] L. PESTOV, V. BOLGOVA, AND O. KAZARINA, *Numerical recovering of a density by the BC-method*, Inverse Probl. Imaging, 4 (2010), pp. 703–712, <https://doi.org/10.3934/ipi.2010.4.703>.

-
- [35] L. PESTOV, G. UHLMANN, AND H. ZHOU, *An inverse kinematic problem with internal sources*, *Inverse Problems*, 31 (2015), pp. 055006, 6, <https://doi.org/10.1088/0266-5611/31/5/055006>.
- [36] W. W. SYMES, *The seismic reflection inverse problem*, *Inverse Problems*, 25 (2009), pp. 123008, 39, <https://doi.org/10.1088/0266-5611/25/12/123008>.
- [37] D. TATARU, *Unique continuation for solutions to pde's; between Hörmander's theorem and Holmgren's theorem*, *Communications in Partial Differential Equations*, 20 (1995), pp. 855–884, <https://doi.org/10.1080/03605309508821117>.
- [38] D. TATARU, *On the regularity of boundary traces for the wave equation*, *Ann. Scuola Norm. Sup. Pisa Cl. Sci. (4)*, 26 (1998), pp. 185–206.